Journal of Engg. Research **Vol. 5 No. (1) March 2017 pp.** *163-180*

مقارنة بين مختلف أساليب المحاكاة العددية للتنبؤ بخسارة الإرسال في كواتم الصوت

لي–شين جو و وي فان

مدرسة الهندسة الميكانيكية والميكنة، جامعة شمال-الشرق، شينيانج، جمهورية الصين الشعبية

الخـلاصــة

مع التطور السريع في أجهزة الكمبيوتر عالية الأداء، شهدت السنوات الأخيرة اهتماما متزايدا في اعتماد أساليب المحاكاة العددية للتنبؤ بخسارة الإرسال (TL) في كواتم الصوت. في هذه الورقة، نقوم بتطبيق طريقتين مختلفتين للمحاكاة العددية على قيم خسارة الارسال (TL) ليتم فحصها، وهي طريقة العناصر المحددة (FEM) ثلاثية الأبعاد (3-D) والطريقة الحسابية لديناميكا الموائع (CFD) في مجال الوقت. تتم مقارنة التنبؤات في قيم (TL) التي تم الحصول عليها من الطريقتين مع النتائج التجريبية والعددية المنشورة. وخلص البحث إلى أنه بوجه عام، فإن الطريقتان تعطيان توقعات معقولة لخسارة الارسال (TL) سواء مع أو بدون التدفق المتوسط. وعلاوة على ذلك، يتم إجراء دراسة مقارنة بين الطريقتين بالنسبة الى معايير الدقة واستهلاك الوقت وسهولة الاستخدام. وتشير النتائج إلى أن طريقة مجال الوقت (CFD) ممكن أن تحقق نتائج أكثر دقة ولكنها تستغرق وقتا طويلا، بينما طريقة العناصر المتناهية (FEM) أسرع بشكل ملحوظ ولكنها مرهقة للاستخدام قليلا.

A comparison between various numerical simulation methods for predicting the transmission loss in silencers

Li-Xin Guo and Wei Fan

School of Mechanical Engineering and Automation, Northeastern University, Shenyang 110819, P. R. China

Corresponding author: lxguo@mail.neu.edu.cn

ABSTRACT

With the rapid development of high-performance computers, recent years have seen an increasing interest in adopting numerical simulation methods to predict the transmission loss (TL) in silencers. In this paper, two different numerical simulation methods applied to the computation of TL values are investigated; namely the three-dimensional (3-D) finite element method (FEM) and the time-domain computational fluid dynamics (CFD) method. TL predictions obtained from the two investigated methods are compared with experimental and numerical results in the published literature, and it is concluded that overall, both methods can be powerful tools to give reasonable predictions for the studied silencers with and without mean flow. Furthermore, a comparative study of the two methods considering the criteria including accuracy, time consumption and ease of use is made. The results presented indicate that the time-domain CFD method can deliver more accurate results, but it is much more time-consuming, and the FEM is significantly faster but a little cumbersome to use.

Key words Mean flow; silencer; three-dimensional finite element method; time-domain computational fluid dynamics method; transmission loss.

NOMENCLATURE

A cross-sectional area (m^2)
c sound velocity (m/s)
d inlet/outlet pipe diameter (mm)
d_h perforate hole diameter (mm)
D expansion chamber diameter (mm)
J mass flux (kg/m^2·s)
k wave number
l silencer length (mm)
l_d distance between downstream monitor point and silencer (mm)
l_u distance between upstream monitor point and silencer (mm)

Greek Letter

δ duration (s)
ρ medium density (kg/m^3)
σ perforated pipe porosity
ω angular frequency

Subscripts

0 constant value
in inlet
inc incident wave
I impulse signal
out outlet
ref reflective wave

L_d length of the downstream pipe

p acoustic pressure (Pa)

TL transmission loss (dB)

T temperature (K)

u particle velocity (m/s)

v flow velocity of the medium (m/s)

x coordinate of the point along the silencer axis

tra transmitted wave

T transmitted signal

INTRODUCTION

The major contribution of silencer is the attenuation of the noise generated by vehicles and fluid machines. Transmission loss (TL) is often used to evaluate the acoustic attenuation performance of a silencer (Beranek & Vér, 1992). For the TL prediction, two numerical simulation methods, namely the frequency-domain method based on the linear acoustic model and the time-domain method based on the non-linear fluid dynamic model (Ji *et al*., 2010), are available.

Frequency-domain method mainly includes the boundary element method (BEM) (Wu *et al*., 2002; Wang, 2007; Park *et al*., 2009; Siano, 2011) and the finite element method (FEM). FEM was initially applied to predict the acoustic performance of silencers by Young & Crocker (1975), and it has been the most common numerical method for TL prediction to date. In the past, researchers often restricted themselves to a 2-D analysis (Craggs, 1976; Rosenhouse & Findling, 1997; Lan *et al*., 2001) with a simplified boundary condition, because of a limit to computational resources. In recent years, with the rapid development of high-performance computers, the applications of 3-D FEM (Mehdizadeh & Paraschivoiu, 2005; Chaitanya & Munjal, 2011; Liu *et al*., 2013; Fu *et al*., 2015), which require higher computation and memory resources are growing rapidly. In most of previous works, the use of 3-D FEM mainly centers on calculating TL in silencers without mean flow. It is well known that the sound propagation in silencers is actually coupled with the mean gas flow, of course, the FEM is capable of considering the effect of mean flow by assuming that the acoustic field is superimposed over the decoupled mean flow (Broath *et al*., 2005), but this mean flow must be imported from an external steady flow computation that is often performed by a simplified potential-flow approach (Peat, 1982) in previous works. In this paper, to acquire more realistic flow distribution inside the silencer, especially for those silencer systems which have complex geometry, a full CFD simulation with proper turbulence model is employed to perform the flow computation, and then the obtained mean flow data are imported to an acoustic solution undertaken using 3-D FEM.

For the time-domain method, the traditional 1-D ones (Chang & Cummings, 1988; Selamet *et al*., 1995; Dickey *et al*., 1998) are based on the assumption of axial 1-D plane wave propagation and only valid for lower frequency acoustic analysis of the silencers (Shaw *et al*., 2003), while realistic silencer geometries often exhibit multi-D features, so these methods are limited in practical application. The 2-D and 3D time-domain methods are also called time-domain CFD method due to the fact that in these methods, the basic equations governing fluid motion are often solved by CFD code. A 2-D axi-symmetric time-domain CFD method is proposed to calculate the TL of simple expansion chamber mufflers without mean flow by Middelberg *et al*. (2004), and their predictions showed very close agreement with published experimental results. Continuing, Broatch *et al*. (2005) developed a time-domain CFD methodology based on 3-D CFD simulation to calculate the acoustic response of simple expansion chamber silencer and reversing chamber silencer, and their predictions presented a good agreement with measurements in the absence of mean flow. Recently, Liu & Ji (2014) applied the 3D time-domain CFD method to investigate the acoustic attenuation performance of straight-through perforated pipe silencers with mean flow, and their results agreed fairly well with experiments. Except for aforementioned works, to the best knowledge of the current authors, very few applications of the time-domain CFD method for TL predictions can be found in the existing literature; so it is necessary to further investigate this method.

This paper focuses mainly on the 3-D FEM and the time-domain CFD method, and a comparison between these two numerical simulation methods is made from the point of view of accuracy, time consumption and ease of use evaluation. Next section gives a detailed description of the investigated methods. Subsequently, the obtained numerical results are presented and compared. Finally, some conclusions are drawn.

NUMERICAL SIMULATION METHODS

Silencers considered

In order to investigate the performance of the numerical simulation methods, some representative silencers are chosen as the illustration examples: (i) single and double circle expansion chamber silencers with extended inlet/outlet used in References (Wang, 2000; Bilawchuk & Fyfe, 2003; Wang, 2007), and (ii) straight-through perforated pipe silencers used in Reference (Lee & Ih, 2003). Also, this paper uses the published experimental data from aforementioned literature as a basis for comparison for the numerical results presented. Figure 1 shows the geometries of the silencers considered here and their precise dimensions are given in Table 1, where d_h and σ denote the diameter of the orifice on the perforated pipe and the porosity, respectively.

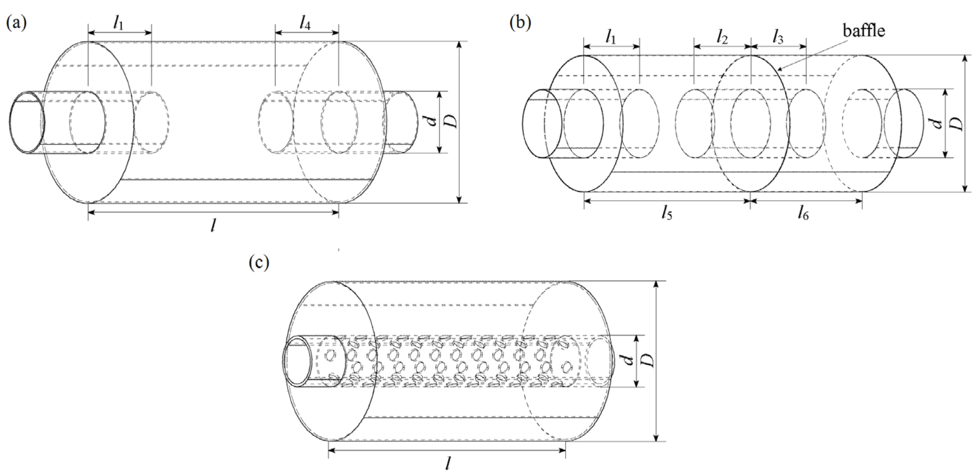

Fig. 1. Geometries of silencers considered: (a) single expansion chamber silencer, (b) double expansion chamber silencer, (c) straight-through perforated pipe silencer

Table 1. Dimensions for the silencers considered (Unit: mm)

Silencer	D	d	l	l_1	l_2	l_3	l_4	l_5	l_6	d_h	σ (%)
Single chamber 1 (S1)	149.3	52.5	453	0	_	_	0	_	_	_	_
Single chamber 2 (S2)	108	40	208	52	_	_	0	_	_	_	_
Single chamber 3 (S3)	108	40	208	52	_	_	52	_	_	_	_
Double chamber (D)	400	200	_	200	200	200	_	600	400	_	_
Perforated pipe 1 (P1)	110	32	200	_	_	_	_	_	_	4	4.7
Perforated pipe 2 (P2)	110	32	200	_	_	_	_	_	_	8	14.7

3-D FEM

As stated in the first section, in this paper the FEM is used in conjunction with the CFD simulation, when mean flow is present in the silencers. The CFD steady flow computation is performed first by means of the commercial software ANSYS FLUENT 14.5, and then the commercial software LMS Virtual.Lab is used to perform the acoustic response analysis in FEM module. The mean flow data transfer between the two procedures is accomplished by mesh mapping function that Virtual. Lab provides (LMS Virtual.Lab Online Help, 2013).

Tetrahedral mesh is chosen to discretize the computational field of the silencer, due to its flexibility in modeling complex structures. Two different meshes are used for the solution of the CFD and acoustic problems. To ensure computational accuracy, the maximum size of the acoustic mesh should be small enough to allow at least six elements to fit in the wavelength of the maximum frequency of interest, and the CFD mesh, is about twice as fine as the acoustic mesh (Yadav *et al*., 2011; LMS Virtual.Lab Online Help, 2013). Take silencer S3 as an example, Figure 2(a) shows its CFD mesh, which is fine and dense and the mesh near to the walls is densified further in order to resolve the boundary layer. Compared with the CFD mesh, the acoustic mesh shown in Figure 2(b) is coarse and thin. Moreover, it can be seen from Figure 2(b) that the mesh near to the walls is not densified further. This is because the accuracy of the solution for the acoustic problem is determined by most of mesh elements, and local mesh refinement cannot improve the accuracy (Zhan & Xu, 2013).

(a) (b)

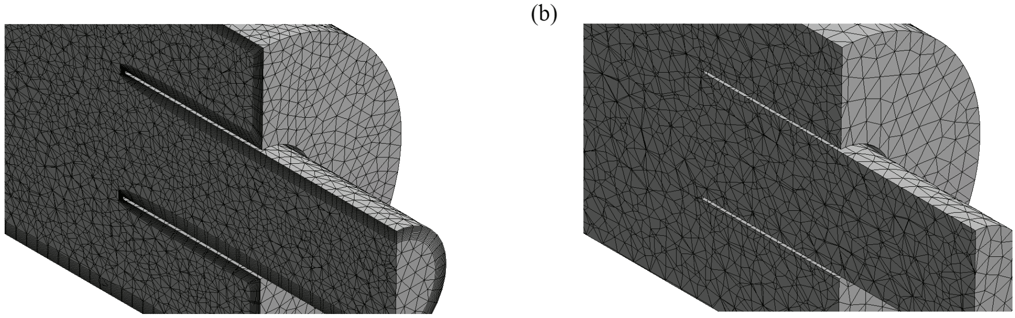

Fig. 2. Meshes for the silencer considered: (a) CFD mesh, (b) acoustic mesh

In the CFD steady flow computation, the data type used is double precision and the solver implemented is a pressure-based implicit solver. SIMPLEC pressure-velocity coupling algorithm is chosen with second order scheme for spatial discretisation, and the realizable k-epsilon turbulence model is employed (ANSYS FLUENT User's Guide, 2012). The fluid is air with the density conforming to the ideal gas law. The boundary conditions consist of: (i) a mass-flow-inlet with constant mass flux, (ii) a pressure-out with constant static pressure, in this case 0 Pa relative to one standard atmospheric pressure, and (iii) the walls assumed to be stationary, with no slip and adiabatic.

After convergence of the CFD steady flow computation, the obtained flow velocity is imported to the acoustic field by mesh mapping, and then used as a mean flow boundary condition of the acoustic response analysis (i.e. the results are superimposed over the acoustic field). Besides, at the inlet face of the silencer, there is a unit velocity of u_{in}=1 m/s, and the outlet is defined to be an anechoic end by setting an Aanechoic end duct property in Virtual.lab. Finally, the acoustic response analysis is performed with 10 Hz spacing using FEM. and the TL is determined by

$$TL = 20\lg\left[\left(\frac{A_{in}}{A_{out}}\right)^{\frac{1}{2}}\left|\frac{p_{inc}}{p_{tra}}\right|\right] \tag{1}$$

where A_{in} and A_{out} are the cross-sectional areas of the inlet and outlet of the silencer, respectively, and p_{inc} is the acoustic pressure of incident wave at the inlet of the silencer, p_{tra} is the acoustic pressure of transmitted wave at the outlet of the silencer (Munjal, 2014). However, it should be pointed out that the results obtained using present FEM are acoustic pressures at the inlet and outlet (p_{in} and p_{out}), which include the acoustic pressure of reflective wave (p_{ref}), as shown in Figure 3, where x represents the coordinate of the point along the silencer axis. Therefore, Equation (1) should be further deduced to build the relationship between p_{in},p_{out} and p_{inc}, p_{tra}.

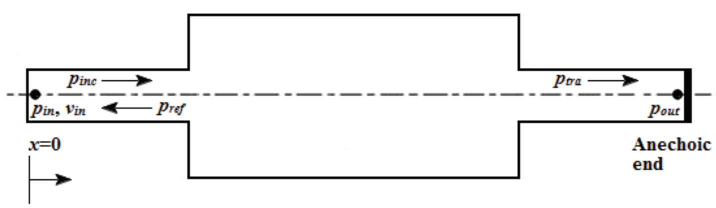

Fig. 3. Theory for TL calculation

In the frequency range of interest for silencer analysis, these acoustic pressure waves typically travel through the inlet and outlet pipes as plane waves (Mehdizadeh & Paraschivoiu, 2005), and when the wave travels in an inviscid moving medium, the 1-D wave formulation is (Munjal, 2014)

$$\frac{\partial^2 p}{\partial t^2} + 2v\frac{\partial^2 p}{\partial x \partial t} + (v^2 - c^2)\frac{\partial^2 p}{\partial x^2} = 0 \tag{2}$$

where p is the acoustic pressure, v is the flow velocity of the medium and c is the sound velocity. By assuming a time-harmonic solution for the acoustic pressure (i.e. assuming the time dependence takes an exponential form), equation (2) is solved to obtain the acoustic pressure at the inlet, which is written as

$$p_{in} = (p_{inc}\mathrm{e}^{-jkx/(1+M)} + p_{ref}\mathrm{e}^{+jkx/(1-M)})\mathrm{e}^{j\omega t} \tag{3}$$

where k is the wave number defined as $k=\omega/c$, ω is the angular frequency, p_{ref} is the acoustic pressure of reflective wave at the inlet, and M is the mean flow Mach number defined as $M=v/c$. The particle velocity at the inlet also satisfies the same wave formulation, one can write

$$u_{in} = \frac{1}{\rho c}(p_{inc}\mathrm{e}^{-jkx/(1+M)} - p_{ref}\mathrm{e}^{+jkx/(1-M)})\mathrm{e}^{j\omega t} \tag{4}$$

where ρ is the density of the medium and ρc represents the characteristic impendence of the medium at the inlet. As mentioned before, there are x=0 and u_{in}=1 m/s at the inlet, and with neglecting "e^{jwt}" item, Equations (3) and (4) reduce to

$$p_{in} = p_{inc} + p_{ref} \tag{5}$$

$$u_{in} = (p_{inc} - p_{ref})/\rho c = 1 \tag{6}$$

which yield

$$p_{inc} = (p_{in} + \rho c)/2 \tag{7}$$

In addition, the outlet is defined to be an anechoic end (i.e. the acoustic pressure of reflective wave at the outlet is 0), so there is

$$p_{tra} = p_{out} \tag{8}$$

Substituting Equations (7) and (8) into Equation (1) yields

$$TL = 10\lg\left[\frac{(p_{in}+\rho c)^2}{4p_{out}^2}\frac{A_{in}}{A_{out}}\right] = 10\lg\left(\frac{(p_{in}+\rho c)\overline{(p_{in}+\rho c)}}{4p_{out}\overline{p_{out}}}\frac{A_{in}}{A_{out}}\right) \tag{9}$$

It should be noted that the obtained acoustic pressure is in frequency domain and therefore has a complex value. In this paper, the temperature and density of the medium (air) are T=288 K and ρ=1.225 kg/m^3, respectively, and the sound velocity in air is c=340 m/s.

Time-domain CFD method

Figure 4 illustrates the model for TL prediction by the time-domain CFD method. The essence of this method is to simulate the experimental process of an impulse technique (Singh & Katra, 1978) for measuring acoustic attenuation performance of a silencer. Accordingly, the basic strategy in the time-domain CFD method is to impose a perturbation (impulse signal) at the inlet of the upstream pipe. The effect of the perturbation at the upstream and downstream monitor points is established using the CFD transient flow computation via software FLUENT, and then the obtained time histories of the acoustic pressures at the two monitor points are converted into incident and transmitted acoustic pressures in the frequency-domain by Fast Fourier Transformation (FFT). Finally, the TL is calculated by Equation (1).

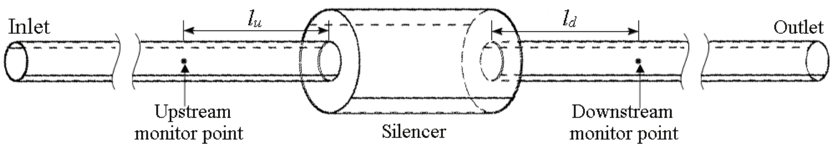

Fig. 4. Scheme for TL prediction using time-domain CFD method

The model has long upstream and downstream pipes, typically 14 times the length of the silencer (Middelberg *et al.*, 2004). Moreover, the locations of the two monitor points must be selected properly so that the isolated incident, transmitted and reflected signals can be captured. For the upstream monitor point, it should capture the incident signal before the reflected signal from the silencer arrives; the downstream monitor point should be located so as to pick up the transmitted signal completely before the reflected signal from downstream pipe termination coming back. Following the suggestions of Singh & Katra (1978), the distances between monitor points and silencer (as shown in Figure 4) should meet

$$l_u > \frac{1}{2}c\left(1-M^2\right)\delta_I \tag{10}$$

$$l_d < L_d - \frac{1}{2}c\left(1-M^2\right)\delta_T \tag{11}$$

where c is the sound velocity, M is the flow velocity in Mach number, L_d is the length of downstream pipe, and δ_I and δ_T represents the durations of impulse signal and transmitted signal, respectively. In addition, the time window (record length of data) should be long enough to capture the entire pressure signals.

To ensure the computational accuracy, the mesh size used for the time-domain CFD method should meet the following requirement. A CFD mesh can resolve a single wavelength corresponding to the maximum frequency of interest with at least 15 mesh points (Middelberg *et al.*, 2004; Xu, 2009). In the CFD transient flow computation, the pressure-velocity coupling algorithm is changed to the PISO algorithm, and the second order scheme is chosen for transient formulation. A half period sinusoid of a frequency of 4000 Hz and a mass flux amplitude of 0.3 kg/m^2·s is used as impulse signal in this study. The inlet boundary is mass-flow-inlet, where the impulse signal is superimposed on a constant mass flux through User-Defined Functions (ANSYS FLUENT User's Guide, 2012) and the time varying mass flow could be expressed as

$$J(t) = \begin{cases} J_0 + 0.3\sin\left(2\pi \cdot 4000t\right), & 0 \le t \le 125\mu s \\ J_0, & t > 125\mu s \end{cases} \tag{12}$$

where J_0 is the constant mass flux (J_0=0, when there is no mean flow in silencer). The rest of the solution setup is the same as that for the CFD steady computation stated in 3-D FEM.

Figure 5 shows the captured acoustic pressure signals at the two monitor points for silencer S1 (J_0=0), and herein l_u=850 mm and l_d=200 mm are chosen for the distances between monitor points and silencer. It is found that the incident and transmitted signals have tended to be stable before reflected signals arrive at the monitor points. In order to separate the incident and transmitted signals from the reflected signals, a rectangular window function is used to cut off the unwanted reflections. Figure 6 shows the isolated incident and transmitted signals. Finally, the incident and transmitted acoustic pressures in frequency domain, as shown in Figure 7, can be acquired by means of FFT.

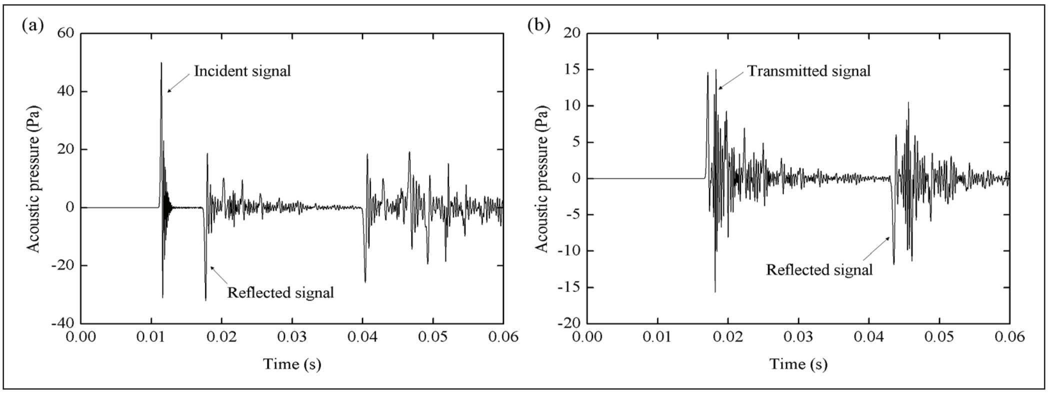

Fig. 5. Time histories of the acoustic pressures at the two monitor points: (a) upstream monitor point, (b) downstream monitor point

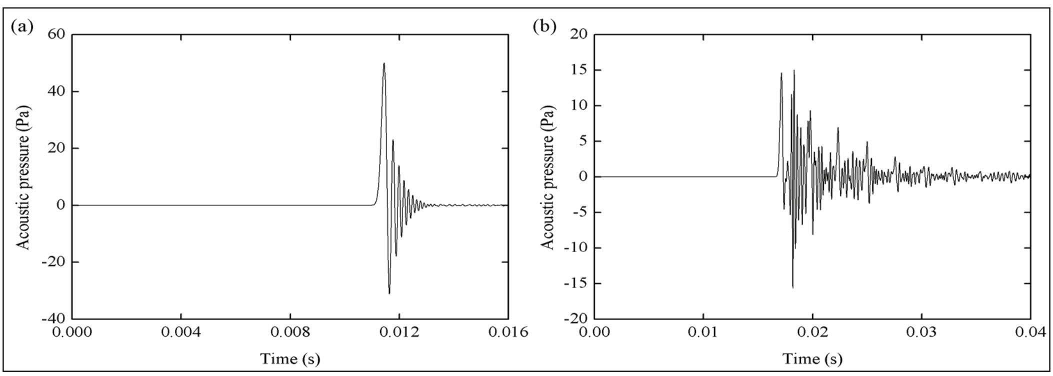

Fig. 6. Isolated acoustic pressure signals: (a) incident signal, (b) transmitted signal

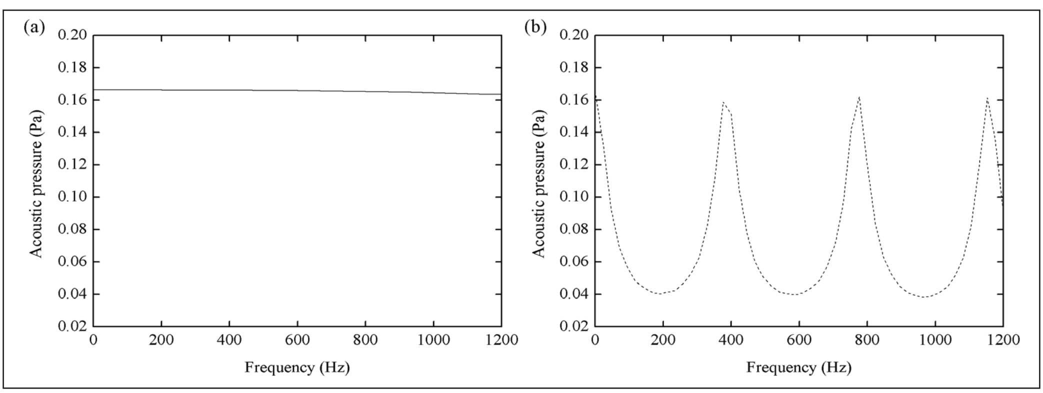

Fig. 7. Acoustic pressures in frequency domain: (a) incident acoustic pressure, (b) transmitted acoustic pressure

When mean flow is present, the CFD transient flow computation with impulse signal is performed first and then the transient computation without impulse signal is run again, and time histories of the static pressures at the monitor points are recorded. The differences between the obtained results from the two transient flow computations are the acoustic pressures in time domain. Additionally, before performing the transient flow computation, the steady flow computation should be initially carried out to acquire the initial distribution of flow field inside the silencer, and subsequently the obtained result from the steady flow computation is used as the initial condition of the transient flow computation. The solution setup of the steady flow computation is the same as that for the CFD computation in 3-D FEM depicted before.

RESULTS AND DISCUSSION

Expansion chamber silencers

When employing 3-D FEM to predict the TL of the expansion chamber silencers with mean flow, CFD steady flow computation should be carried out first, and the element sizes of the CFD meshes are 4 mm and 15 mm respectively for the single and double chamber silencers. Figure 8 illustrates the details of the mean flow inside the silencers with inlet flow velocity of v=10.2 m/s or v=17 m/s, and it is found that the flow velocity distribution is non-uniform, that is to say, there is no a uniform velocity for different locations inside the silencer. The velocity magnitude in the pipe is higher than that in the chamber. The obtained mean flow velocity is exported into format CGNS (CFD General Notation system), so that it may be imported to the acoustic field. Next, acoustic response analysis is performed, and the element sizes of the acoustic meshes are 8 mm and 20 mm respectively for the single and double chamber silencers. The maximum achieved frequencies of the acoustic meshes can be computed in Virtual.Lab, which are 3915.2 Hz, 4311.6 Hz, 4225.6 Hz and 1622.0 Hz respectively for silencer S1, S2, S3 and D; well over the maximum frequency of interest.

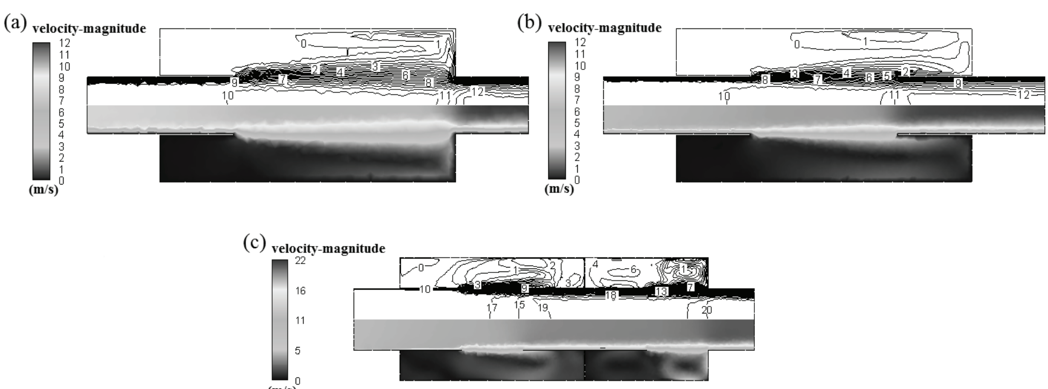

Fig. 8. Counters of velocity magnitude for the expansion chamber silencers: (a) silencer S2, v=10.2 m/s, (b) silencer S3, v=10.2 m/s, (c) silencer D, v=17 m/s

Taking the axi-symmetry properties of the expansion chamber silencers into consideration, when the time-domain CFD method is employed to predict the TL, a 2-D axi-symmetric model is used in the CFD transient flow computation so as to reduce the computational cost. For the single chamber silencer, the lengths of both upstream and downstream pipes are 5000 mm, and the two monitor points are appropriately placed on the axi-symmetric axis (l_u=850 mm, l_d=200 mm). The computational field is discretized with a rectangular mesh of 4 mm. Figure 9 shows the mesh model for silencer S1, which is uniform and consists of 18543 nodes and 16392 elements. For the double chamber silencer, the lengths of both upstream and downstream pipes are 20000 mm and there are l_u=1800 mm, l_d=120 mm. The computational field is discretized with a rectangular mesh of 10mm, and it consists of 32877 nodes and 29960 elements. The time step sizes of the CFD transient flow computations for the single and double chamber silencers are 5 μs and 20 μs, respectively, and their corresponding sampling frequencies are 200 kHz and 50 kHz, both of which are much higher than the maximum frequency of interest, so the Nyquist sampling law can be satisfied. The time windows are 0.06 s and 0.03 s respectively for the single and double chamber silencers. Accordingly, 12,000 and 1500 time steps, respectively, for the single and double chamber silencers need to be run in the CFD transient flow computations.

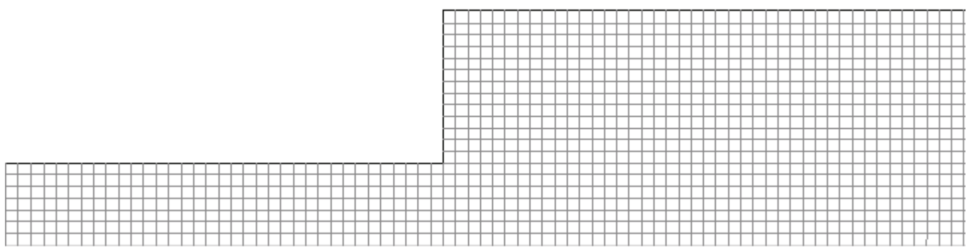

Fig. 9. Mesh used in the time-domain CFD method

Figure 10 compares the predicted and experimental measured TL curves for the expansion chamber silencers in the absence of mean flow. It can be seen that both predictions from the CFD and FEM show excellent agreements with the measurements. In addition, it is found that the TL curves of silencer D calculated by the CFD method are not smooth and have some saw teeth. This is due to the fact that the time-domain CFD method is a simulation of the process of an impulse technique for measuring silencer acoustic performance and therefore the predicted TL curves are easy to fluctuate like those obtained from the impulse technique.

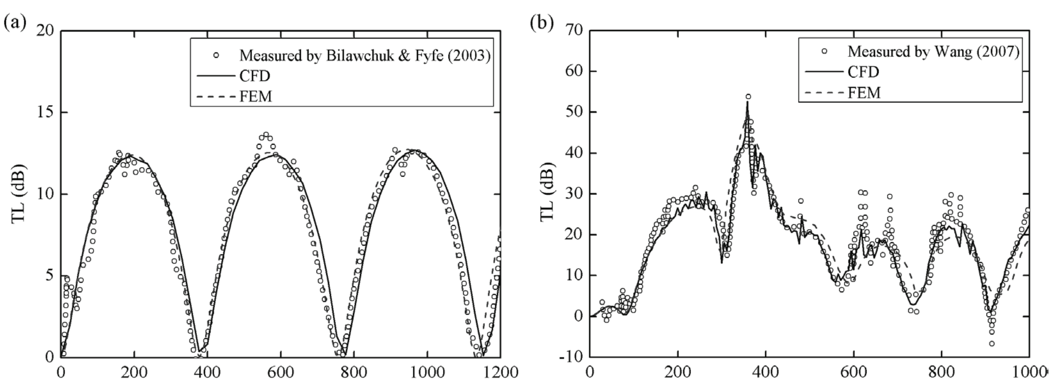

Fig. 10. A TL comparison between different numerical simulation methods and experimental measurement: (a) silencer S1, v=0, (b) silencer D, v=0

In Figure 11 predictions are compared against measurements for the silencers with mean flow, and it should be pointed out that, as with the FEM, both methods used in References (Wang, 2000; Wang, 2007) belong to the frequency-domain method and consider the mean flow effect based on a potential-flow assumption. One can observe that the time-domain CFD method yields the best results among the predictions, and the slight difference from experimental result is assessed in relation to the neglected flow noise. This is to be expected because the influence of mean flow on the acoustic attenuation performance of the silencer may be explained as convective and dissipative effects (Ji *et al*., 2010), both of which can be taken into account by the time-domain CFD method, and accurate results may be obtained. Also, it should be noted that, for all the TL curves predicted by the FEM and cited literature, the peak value of the second major arch does not follow up with that measured. This discrepancy may be due to lack of consideration of dissipative effect of medium viscous in these frequency-domain methods, and the dissipative effect is enhanced as mean flow velocity increasing, thus causing more sound energy loss and changing the TL. Furthermore, a comparison between the present FEM and cited previously numerical methods shows that the accuracy of the FEM is higher. That may be because the methods employed in the literature neglect the turbulence (induced by the sudden change of section area) inside the silencers and use simplified mean flow velocity. In contrast, the present FEM may acquire more realistic mean flow distribution through the CFD steady flow computation with proper turbulence model.

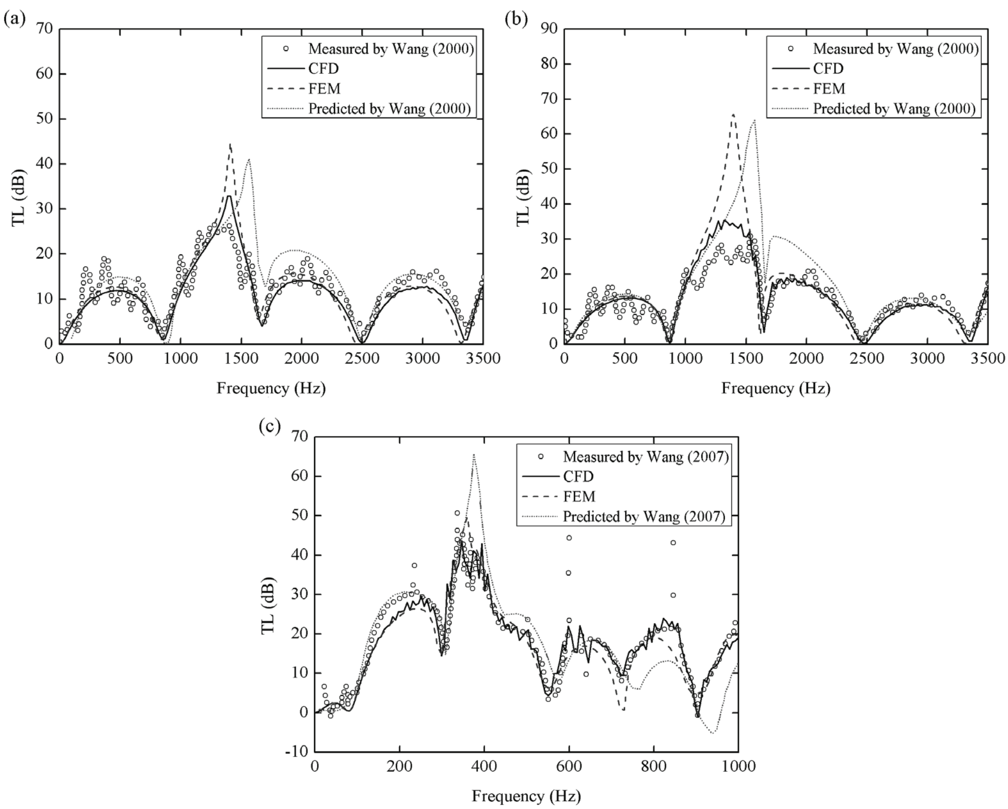

Fig. 11. A TL comparison between different numerical simulation methods and experimental measurement: (a) silencer S2, v=10.2 m/s, (b) silencer S3, v=10.2 m/s, (c) silencer D, v=17 m/s

Figure 12 shows the computation time of the TL predictions illustrated in Figure 10 (a) and Figure 11 by means of the investigated numerical simulation methods. It is vividly depicted in the figure that although the axi-symmetry properties of the silencers has been exploited to decrease the computational cost in the time-domain CFD method, its time consumption is still much higher than that of the FEM using the full 3-D model. Additionally, for the time-domain CFD method, the time consumption of the CFD transient flow computation with impulse signal is nearly the same as that without impulse signal. For 3-D FEM, the time consumption of CFD steady flow computation is higher than that of acoustic response analysis and takes up almost 80 percent of the entire computation time, as shown in Figure 13. Overall, the accurate results of the CFD simulation are obtained at the expense of high time consumption. Recently, in order to decrease the computational effort of the time-domain CFD method, some modified impulse methods have been proposed (Torregrosa *et al*., 2012) and non-reflecting boundary condition (NRBC) is applied at the inlet and outlet of the computational model to reduce the length of upstream and downstream pipes, and good agreements are presented between the predictions and experimental data. However, some tiny spurious reflections still existed under the condition of the improved NRBCs. Therefore, to exclude the effect of spurious reflections, the NRBC isn't employed in present work.

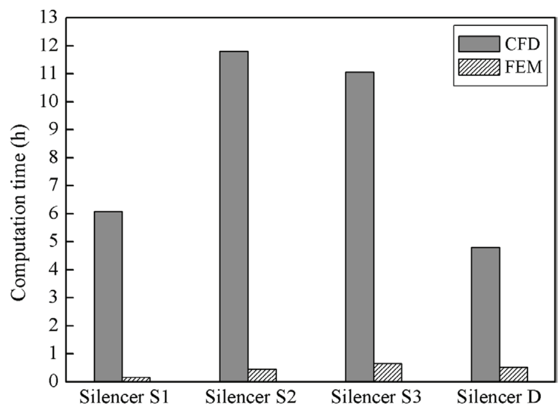

Fig. 12. Comparison of computation time for the time-domain CFD method and 3-D FEM

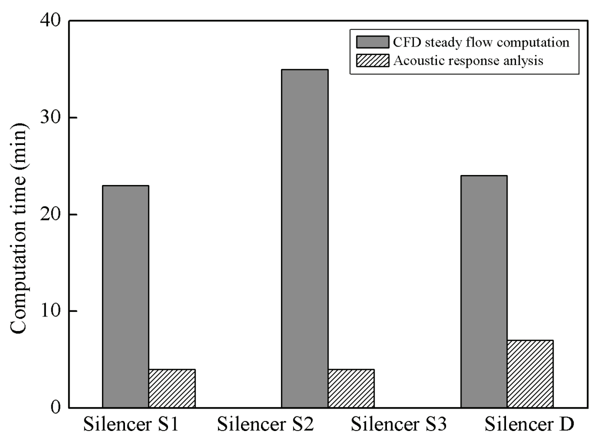

Fig. 13. Comparison of computation time for the CFD steady flow computation and acoustic response analysis in 3-D FEM

In terms of ease of use, the differences between the time-domain CFD method and 3-D FEM are minor. The FEM, however, is a little more cumbersome to be used due to the fact that two different meshes (CFD mesh and acoustic mesh) are required when mean flow is present, and the CFD steady flow computation needs to be performed separately from the acoustic response analysis. The setup of the time-domain CFD method is a little easier and faster than that of the FEM, but compared to the entire computation time required, this difference may be neglected. Moreover, data processing in the time-domain CFD method is more complex.

Straight-through perforated pipe silencers

To further verify the accuracy of the investigated numerical simulation methods, the predicted and measured TL is compared for the straight-through perforated pipe silencers, whose structures are more complex. Because Liu & Ji (2014) have predicted the acoustic attenuation performance of the studied silencers using the time-domain CFD method, we quote their results directly and calculate the TL only with 3-D FEM in this work.

In order to decrease the computational cost, the computational field is split into several parts to generate tetrahedral mesh individually, when employing the FEM. The element sizes of the regions near the perforation for both CFD and acoustic meshes are 2 mm, and the element sizes are 4 mm and 10 mm respectively for the rest of parts of the CFD and acoustic meshes. Figure 14 shows the axial cutting planes of the generated 3-D meshes for silencer P2, and the CFD and acoustic meshes are composed of about 1,000,000 elements and 50,000 elements, respectively. The maximum achieved frequencies of both silencer P1 and P2 are above 3500 Hz; well over the maximum frequency of interest (3000 Hz).

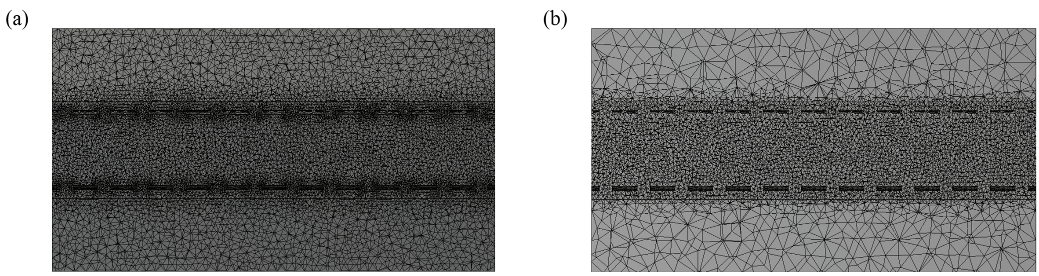

Fig. 14. Meshes used in 3-D FEM: (a) CFD mesh, (b) acoustic mesh

Figure 15 depicts the velocity vector distributions in the perforated pipe silencers. Flow circulations can be observed in the rear part of the silencer, and the velocity in the pipe is much higher than that in the orifices and chamber. Overall, the flow velocity distribution inside the silencer is anisotropic and non-uniform. In addition, under the action of pressure difference between the chamber and perforated pipe, the gas flows into the chamber through the orifices and then flows back again into the pipe, which enhances the turbulent kinetic energy near the orifices, as shown in Figure 16.

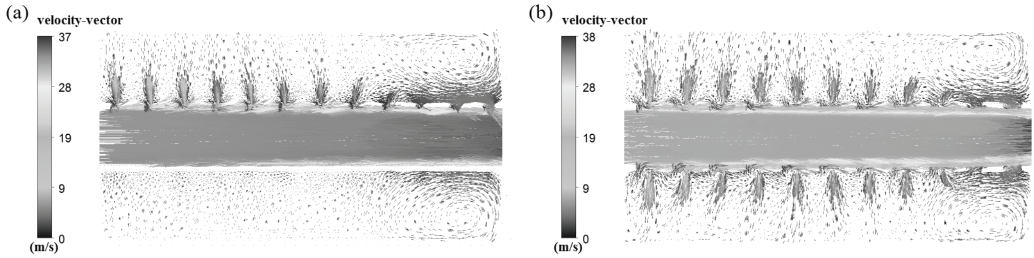

Fig. 15. Velocity vectors for the straight-through perforated pipe silencers: (a) silencer P1, M=0.1, (b) silencer P2, M=0.1

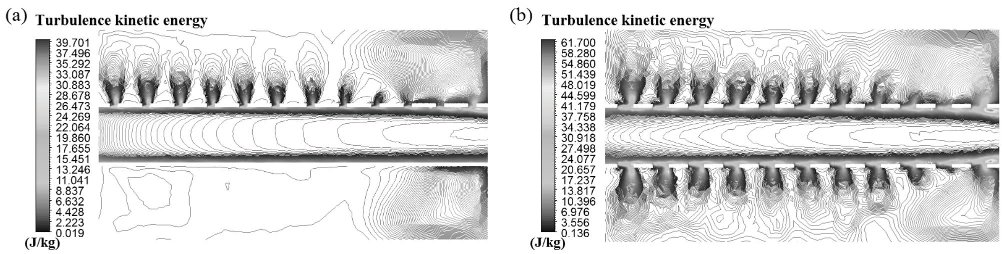

Fig. 16. Counters of turbulent kinetic energy for the straight-through perforated pipe silencers: (a) silencer P1, M=0.1, (b) silencer P2, M=0.1

In Figure 17, the predictions from the 3-D FEM and the time-domain CFD method are reported and compared with the published experimental and numerical results given by Lee & Ih (2003), where the TL of the perforated pipe silencer is predicted with the help of an empirical perforate impedance model in grazing mean flow. It is found that the time-domain CFD method still yields the best results among the predictions. Also, the results of the FEM agree well with the experimental data, and the discrepancy may be attributed to lack of consideration of dissipative effect of medium viscous. In addition, it should be pointed out that by decoupling the acoustics from the mean flow computations, it is fine for the general linear acoustics problem away from the perforation, but the complex phenomena that can happen at perforation, such as the possibility of violent interaction between the acoustic field and the mean flow field, cannot be included, thus lowering the computational accuracy. Similarly, the numerical results from the cited literature are not as accurate as that predicted by the time-domain CFD method. Maybe the reason is that when mean flow is present, rigorous mathematical modeling of the mechanisms that determine the acoustic impedance of a perforate is extremely difficult, so most of current impedance models considering the mean flow effect are empirical ones, which may not be obtained accurately in the presence of complex mean flow. In contrast, the time-domain CFD method may simulate the perforation directly, and account for the nonlinear dissipative effect associated with the interaction between the acoustic and flow fields by using the proper turbulence model in the CFD transient flow computation. That is, the effects of the complex flow and medium viscosity on the sound propagation inside the silencers can be included. Therefore, it is no surprise that more accurate results can be obtained using the time-domain CFD method. For the present 3-D FEM that used in conjunction with the CFD when mean flow is present, although there is a lack of consideration of mean flow dissipative effect on sound propagation, its accuracy is acceptable enough.

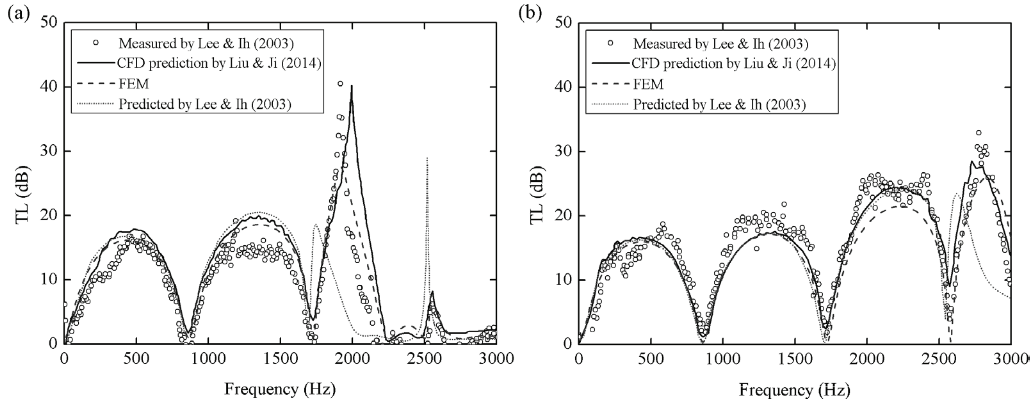

Fig. 17. A TL comparison between different numerical simulation methods and experimental measurement: (a) silencer P1, M=0.1, (b) silencer P2, M=0.1

CONCLUSIONS

Two numerical simulation methods, namely time-domain CFD method and 3-D FEM, are presented for the prediction of the TL in circle expansion chamber silencer and straight-through perforated pipe silencer, and compared here. The following conclusions can be drawn.

The time-domain CFD method may include the complex flow and medium viscosity effects on silencer acoustic attenuation performance, and therefore it is capable of delivering significantly accurate predictions for all studied silencers. The major drawback of the time-domain CFD method lies in the very high computational cost, that is, considerable computation time is required to acquire a complete and accurate solution.

The 3-D FEM is as accurate as the time-domain CFD method in the absence of mean flow. When mean flow is present, the FEM is used in conjunction with CFD simulation in this paper, although the accuracy of the FEM is lower than the time-domain CFD method due to lack of consideration of dissipative effect of mean flow, the FEM is significantly faster and the numerical predictions presented are acceptable and not bad.

In terms of ease of use, the differences between the time-domain CFD method and 3-D FEM are minor. The present FEM is a little cumbersome to use, when mean flow is present, because it requires two different meshes to perform the CFD steady flow computation and acoustic response analysis, respectively. The setup of the time-domain CFD method is a little easier and faster, but the data processing is more complex.

ACKNOWLEDGMENTS

This research received the grants from the National Natural Science Foundation of China (51275082, 11272273) and the Program for Liaoning Innovative Research Team in University (LT2014006)).

REFERENCES

ANSYS FLUENT Version 14.5 User's Guide. 2012. ANSYS INC.

Beranek, L.L. & Vér, I.L. 1992. Noise and vibration control engineering: Principles and applications. Wiley, New York, USA.

Bilawchuk, S. & Fyfe, K.R. 2003. Comparison and implementation of the various numerical methods used for calculating transmission loss in silencer systems. Applied Acoustics, **64**(9):903-16.

Broatch, A., Margot, X., Gil, A. & Denia, F.D. 2005. A CFD approach to the computation of the acoustic response of exhaust mufflers. Journal of Computational Acoustics, **13**(2):301-16.

Chaitanya, P. & Munjal, M.L. 2011. Effect of wall thickness on the end corrections of the extended inlet and outlet of a double-tuned expansion chamber. Applied Acoustics, **72**(1):65-70.

Chang, I.J. & Cummings, A. 1988. A time domain solution for the attenuation, at high amplitudes, of perforated tube silencers and comparison with experiment. Journal of Sound and Vibration, **122**(2): 243-59.

Craggs, A. 1976. A finite element method for damped acoustic systems: An application to evaluate the performance of reactive mufflers. Journal of Sound and Vibration, **48**(3):377-92.

Dickey, N.S., Selamet, A. & Novak, J.M. 1998. Multi-pass perforated tube silencers: a computational approach. Journal of Sound and Vibration, **211**(3):435-47.

Fu, J., Chen, W., Tang, Y., Yuan W.H., Li, G.M. & Li, Y. 2015. Modification of exhaust muffler of a diesel engine based on finite element method acoustic analysis. Advances in Mechanical Engineering **7**(4): 1687814015575954.

Ji, Z.L., Xu, H.S. & Kang, Z.X. 2010. Influence of mean flow on acoustic attenuation performance of straight-through perforated tube reactive silencers and resonators. Noise Control Engineering Journal, **58**(1):12-7.

Lan, J., Shi, S.X. & Hao, Z.Y. 2001. Study on the calculation of the acoustical transfer property of exhaust muffler. Transactions of Csice, **19**(3):275-8.

Lee, S.H. & Ih, J.G. 2003. Empirical model of the acoustic impedance of a circular orifice in grazing mean flow. Journal of the Acoustical Society of America, **114**(1):98-113.

Liu, C., Ji, Z.L. & Fang, Z. 2013. Numerical analysis of acoustic attenuation and flow resistance characteristics of double expansion chamber silencers. Noise Control Engineering Journal, **61**(5):487-99.

Liu, C. & Ji, Z.L. 2014. Computational fluid dynamics-based numerical analysis of acoustic attenuation and flow resistance characteristics of perforated tube silencers. Journal of Vibration and Acoustics-Transaction of the ASME, **136** (2):021006.

LMS Virtual.Lab Version 11-SL2 Online Help. 2013. LMS International NV.

Mehdizadeh, O.Z. & Paraschivoiu, M. 2005. A three-dimensional finite element approach for predicting the transmission loss in mufflers and silencers with no mean flow. Applied Acoustics, **66**(8):902-18.

Middelberg, J.M., Barber, T.J., Leong, S.S., Byrne, K.P. & Leonadi, E. 2004. CFD Analysis of the acoustic and mean flow performance of simple expansion chamber mufflers. ASME International Mechanical Engineering Congress and Exposition, Anaheim, USA.

Munjal, M.L. 2014. Acoustic of Ducts and Mufflers. Wiley, New York, USA.

Park, Y.B., Ju, H.D. & Lee, S.B. 2009. Transmission loss estimation of three-dimensional silencers by system graph approach using multi-domain BEM. Journal of Sound and Vibration, **328**(4-5):575-85.

Peat, K.S. 1982. Evaluation of four-pole parameters for ducts with flow by the finite element method. Journal of Sound and Vibration, **84**(3):389-95.

Rosenhouse, G. & Findling, O. 1997. Computational and physical aspects in cells mufflers design. 2nd International Conference on Computational Acoustics and Its Environmental Applications. Acquasparta, Italy.

Selamet, A., Dickey, N.S. & Novak, J.M. 1995. A time-domain computational simulation of acoustic silencers. Journal of Vibration and Acoustics-Transaction of the ASME **117**(3A): 323-3l.

Shaw, C.E., Moenssen, D.J. & Kostun, J.D. 2003. A correlation study of computational techniques to model engine air induction system response including BEM, FEM and 1D methods. SAE paper 2003-01-1644, USA.

Siano, D. 2011. Three-dimensional/one-dimensional numerical correlation study of a three-pass perforated tube. Simulation Modelling Practice and Theory, **19**(4):1143-53.

Singh, R. & Katra, T. 1978. Development of an impulse technique for measurement of muffler characteristics. Journal of Sound and Vibration, **56**(2):279-98.

Torregrosa, A.J., Fajardo, P., Gil, A. & Navarro, R. 2012. Development of non-reflecting boundary condition for application in 3D computational fluid dynamics codes. Engineering Applications of Computational Fluid Mechanics, **6(**3):447-60.

Wang, C.N. 2000. A boundary element analysis for simple expansion silencers with mean flow. Journal of the Chinese Institute of Engineers, **23**(4):529-36.

Wang X.R. 2007. Studies of boundary element methods for acoustic performance prediction of marine engine exhanst silencers and experiments. PhD Thesis, Harbin Engineering University, China.

Wu, T.W., Cheng, C.Y.R. & Zhang, P. 2002. A direct mixed-body boundary element method for packed silencers. Journal of the Acoustical Society of America, **111**(6):2566-72.

Xu, H.S. 2009. Study on time-domain simulation and experimental measurement of acoustic performance of exhaust silencers. MD Thesis, Harbin Engineering University, China,

Yadav, P.S., Gaikwad, A.A, Kunde, S. A. & Karanth, N. V. 2011. Prediction of muffler radiated noise for a diesel engine. SAE Paper 2011-26-0065, USA.

Young, C.I.J. & Crocker, M.J. 1975. Prediction of transmission loss in mufflers by the finite-element method. Journal of the Acoustical Society of America, **57**(1):144-8.

Zhan, F.L. & Xu, J.W. 2013. Virtual.Lab Acoustics simulation from entry to master. Northwestern Polytechnical University Press, Xian, China.